

**MULTIPURPOSE SATELLITE BUS (MPS)**

**NAVAL POSTGRADUATE SCHOOL**

531-18  
160607  
P. 10

The Naval Postgraduate School Advanced Design Project sponsored by the Universities Space Research Association Advanced Design Program is a multipurpose satellite bus (MPS). The design was initiated from a Statement of Work (SOW) developed by the Defense Advanced Research Projects Agency (DARPA). The SOW called for a "proposal to design a small, low-cost, lightweight, general purpose spacecraft bus capable of accommodating any of a variety of mission payloads. Typical payloads envisioned include those associated with meteorological, communication, surveillance and tracking, target location, and navigation mission areas." The design project investigates two dissimilar missions, a meteorological payload and a communications payload, mated with a single spacecraft bus with minimal modifications. The MPS is designed for launch aboard the Pegasus Air Launched Vehicle (ALV) or the Taurus Standard Small Launch Vehicle (SSLV).

**MISSION PAYLOADS**

Two payloads were furnished from the MPS bus design, each with distinct mission requirements. The first payload is the Advanced Very High Resolution Radiometer (AVHRR). The AVHRR is an operational radiometer that scans the Earth's surface 24 hours each day in the spectral regions from 0.7 to 12  $\mu\text{m}$ . The AVHRR can provide land, water, and cloud imaging; sea surface temperature; and ice concentration and coverage in either high- or low-resolution modes.

The AVHRR will be launched by the Pegasus Air Launched Vehicle (ALV) into a 833-km (450 n.m.), 0830 descending or 1530 ascending Sun-synchronous orbit at a 98.75° inclination. Orbit period is 101 min with worst case 37-min eclipse occurring during the summer. Average eclipse time is on the order of 33 min. The AVHRR is mounted on the Earth face so that the bus is nadir pointing. Solar array damage due to radiation and orbit altitude degradation are negligible at 833 km (450 n.m.). Figure 1 shows the AVHRR payload configuration.

The second payload considered in the design is the Extremely High Frequency (EHF) communication payload. The EHF payload will supplement existing communications of the operational forces in time of crisis. Communication is done at 2400 bps by means of 32 channels using frequency hopping over 255 frequencies. The signal bandwidth of a single channel is 245 kHz. Total bandwidth required is 2 GHz. The payload was designed to be quickly mated with the MPS bus. The antenna/feed horn arrangement was designed and provided by Lincoln Laboratory.

The EHF communication payload is to be launched by the Taurus Standard Small Launch Vehicle (SSLV) into a 6-8-, or 12-hr Molniya-type orbit. For this design, an 8-hr Molniya-type orbit was chosen with a 500-km (270 n.m.) perigee and a 27,000-km (14,578 n.m.) apogee. Worst-case eclipse for this orbit is 52 min. The EHF payload consists of a 0.81 m  $\times$  0.71 m  $\times$  0.15 m (32 in  $\times$  28 in  $\times$  6 in) structural box that supports the EHF antenna structure and houses the EHF receiver/transmitter and the telemetry, tracking, and command (TT&C) equipment. The EHF and TT&C antennas and the Earth sensor are located on the Earth face of this box, which is affixed to the Earth face of the MPS bus. Optical solar reflectors are mounted on the north face of the structural box and provide radiation of heat of the traveling wave tube amplifiers (TWTA). Figure 2 shows the EHF payload.

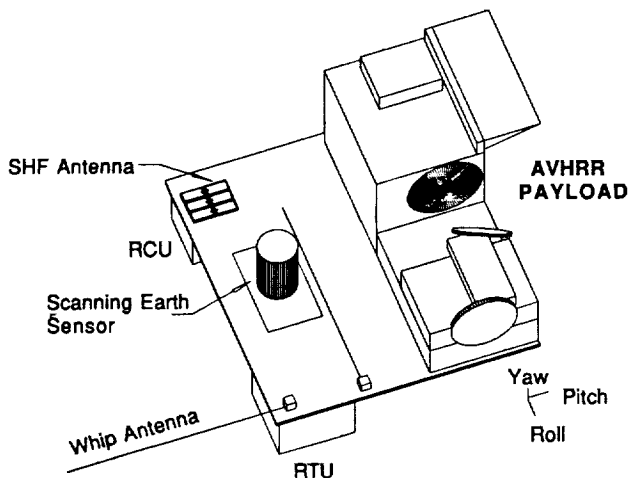


Fig. 1. Earth face with AVHRR payload.

**SPACECRAFT BUS CONFIGURATION**

The two payloads mentioned were suggested by the Defense Advanced Research Projects Agency (DARPA) as typical payloads for this spacecraft. DARPA also expressed in the Statement of Work (SOW) that the spacecraft be compatible with both the Pegasus Air Launched Vehicle (ALV) built by Orbital Sciences Corporation and Hercules Aerospace Company and the Taurus Standard Small Launch Vehicle (SSLV) also built by Orbital Sciences Corporation. The SOW requires that the spacecraft have a design life of three years.

A preliminary design of this MPS bus was performed employing as much modularity as possible. The MPS is a three-axis stabilized satellite with silicon solar-cell panels and nickel-hydrogen (NiH<sub>2</sub>) batteries for power, and hydrazine propulsion. Thermal

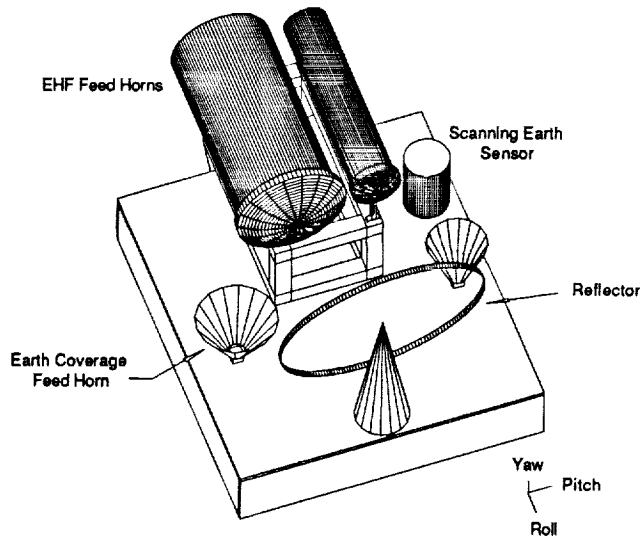


Fig. 2. EHF payload.

control is passive, using optical solar reflector (OSR) material, conductive paths, insulation, paints, and coatings. Detailed analysis was done in the areas of orbit analysis, electrical power, attitude control, thermal analysis, propulsion, telemetry, tracking and control, and structure design.

The MPS bus is designed to allow attachment of various payloads to the Earth face. Modular subsystem components allow the addition or enhancement of MPS performance. The attitude control subsystem, for example, has a precision sensor subsystem (PSS) to augment the basic sensor subsystem (BSS) allowing greater pointing accuracy from  $0.5^\circ$  to  $0.01^\circ$  depending on the mission requirements. The bus as shown in Fig. 3, is a 122.5-kg (270 lb) rectangular box with all the subsystems necessary to fly a variety of orbits and missions.

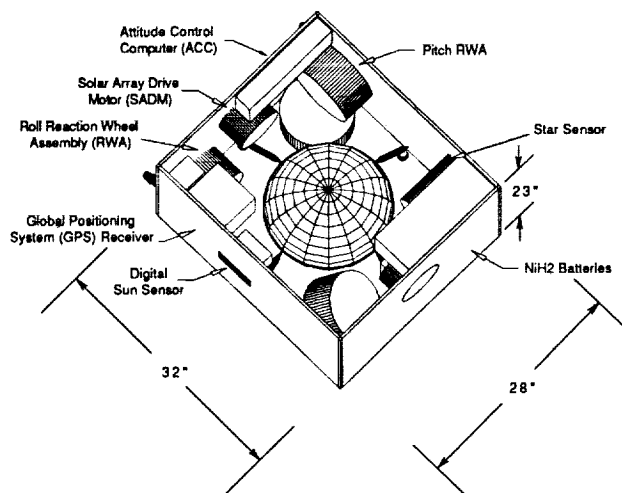


Fig. 3. Multipurpose satellite bus configuration.

**Pegasus Air Launched Vehicle (ALV)**

The Pegasus ALV is a three-stage, solid-propellant, winged rocket designed for the insertion of small payloads into orbit. The 15.2-m (50 ft) long, 1.278-m (50 in) diameter booster weighs 19,052 kg (42,000 lb) and is carried aloft by a conventional transport/bomber-class aircraft (B-52, B-747, L-1011). The payload capability for the ALV is shown in Fig. 4.

**Taurus Standard Small Launch Vehicle (SSLV)**

Taurus is a four-stage, inertially-guided, three-axis stabilized, solid-propellant launch vehicle. The design incorporates a Pegasus first, second, and third stage on a Peacekeeper booster. Taurus is fully transportable with rapid launch site establishment. Initial performance estimates are described in Table 1.

The Taurus SSLV will be required to launch the EHF payload into its 8-hr Molniya orbit because of the additional lift not available from the ALV. The 1.27-m (50 in) diameter  $\times$  2.28-m (90 in) long dynamic envelope of the shroud allows for the addition of a third solar array panel per side if needed [the 1.17-m (46 in) diameter Pegasus shroud allowing only two panels per side]. Two solar arrays are sufficient for the two payloads under this study.

**ORBIT ANALYSIS**

Table 2 contains orbit parameters of the two payloads. Argument of perigee is undefined for the AVHRR orbit since it is circular. A highly inclined orbit results from the required global coverage and low altitude. Careful selection of the inclination produces a Sun-synchronous orbit. Finally, spacecraft currently performing missions similar to the AVHRR mission locate their ascending nodes within a couple of hours of the Earth's terminator (the line that separates the sunlit side from the dark side). This design also finds ascending node within two and a half hours of the terminator.

Parameters of the EHF payload orbit are also summarized in Table 2. The EHF communication mission requires a Molniya-type orbit. An 8-h Molniya-type orbit was selected. The EHF communication mission addresses the deficiency of geosynchronous communication satellites to provide high-latitude

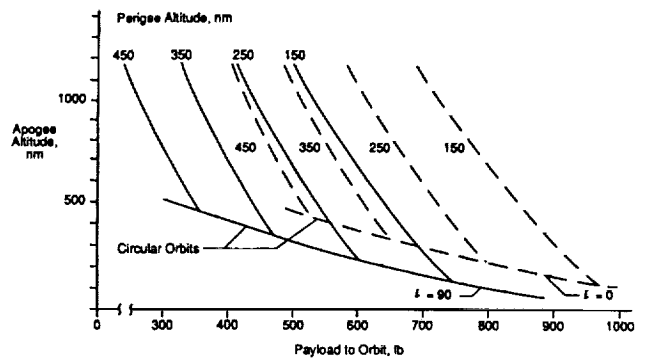


Fig. 4. Pegasus ALV launch capability<sup>(3)</sup>.

TABLE 1. Molniya-type orbits for SSLV ballasted vehicle.

Perigee	Apogee	Period	Payload	Enhanced
500 km (270 n.m.)	39,632 km (21400 n.m.)	12 hrs	88 kg (194 lb)	208 kg (458 lb)
500 km (270 n.m.)	27,360 km (14773 n.m.)	8 hrs	123 kg (277 lb)	260 kg (573 lb)
500 km (270 n.m.)	20,270 km (10945 n.m.)	6 hrs	164 kg (362 lb)	315 kg (694 lb)
500 km (270 n.m.)	12,330 km (6658 n.m.)	4 hrs	246 kg (542 lb)	432 kg (953 lb)

TABLE 2. Summary of orbital parameters.

Payload	AVHRR	EHF Communications
Orbit Type	Sun-synchronous	Molniya
Period	101.5 min	8 hr
Semi-major Axis	7212 km (3894 n.m.)	20,307 km (10,965 n.m.)
Eccentricity	0.0	0.661
Inclination	98.75°	63.43°
Ascending Node	3:30 PM/8:30 PM	N/A
Argument of Perigee	N/A	270°

coverage. A highly inclined, very eccentric orbit was studied with perigee located at the southernmost point in the orbit. The high eccentricity yields a longer loiter time over the northern hemisphere (nearly 90%). The choice of inclination was based on the critical inclination to remove rotation of the line of apsides. This minimizes the effects of perturbations on the orbital elements making the orbit easier to maintain. Although perigee is at 270°, it can be located at 90° if the extreme southern latitudes are of interest. Northern hemisphere coverage is assumed for this design.

Orbit selection for both missions was designed to eliminate orbit maintenance requirements. The Defense Meteorological Satellite Program (DMSP) uses the same orbit as the AVHRR mission. SMSP has several payloads, one of which is very similar to the AVHRR. DMSP performs no orbit maintenance during its lifetime.

The EHF payload orbit was analyzed for zonal harmonics  $J_2$  through  $J_7$ , resulting in a 500-yr period for rotation of the perigee. Perigee will move less than 2.5° for the satellite's mission life. The changes in inclination and eccentricity over the satellite's lifetime are also very small.

#### AVHRR Payload Mission

The AVHRR mission is Sun-synchronous, with the longitude of the ascending node move along the Earth's equator rather than remaining fixed in inertial space. The longitude of the ascending node travels once around the equator in one year. If the plane of the equator and the plane of the ecliptic were coplanar, then the Sun would remain in the same relative location with respect to the orbit. Since they are not coplanar, the location of the Sun depends on the season. The AVHRR orbit analysis was directed at determining Sun angles on the satellite, Sun angles on the solar arrays, and eclipse periods.

The primary motivation for this analysis is to ensure that the placement of the AVHRR payload on the spacecraft will prevent sunlight from shining in the sensor field of view and to prevent illumination of the thermal radiator. The basic approach is to define vectors normal to each of the satellite's faces. These vectors are the roll, pitch, and yaw axes and their negatives. Another vector is defined to point from the satellite directly at the Sun. The angle of incidence of sunlight striking a satellite face is the angle between the Sun vector and the vector normal to the satellite face. This angle shall be referred to as the Sun angle of a particular face. If the Sun angle is 0°, then the Sun is shining directly on the satellite face. If the Sun angle is greater than 90°, then the satellite face is oriented away from the Sun and has no incident sunlight.

The orbit is assumed fixed in inertial space for the period of one orbit. The angle between the Sun vector and the orbit normal vector is then a constant. The Sun angle on the satellite's pitch face and negative pitch face also remains constant for that orbit since the satellite's pitch axis is parallel to the orbit normal vector. The Sun angles on the remaining four faces vary as shown in Fig. 5 for the first day of winter. All four faces experience the same Sun angle profile, but shifted in time. The orbit's ascending node is at 8:30 p.m.

The plots for the other seasons are similar in general shape but contain a phase shift and a change in amplitude. Figure 6 examines the Sun angle profile on the +roll face for the first day of all four seasons.

A second study involves the solar array Sun angle over the orbit and the required rotation angle to minimize the solar array Sun angle. Rotation of the solar arrays only provides two locations in each orbit where the resulting solar array Sun angle is zero. Figure 7 shows the seasonal solar array rotation angles. Figure 8 illustrates the worst-case solar array Sun angles over a year. Rotation angle profiles will be required either by onboard

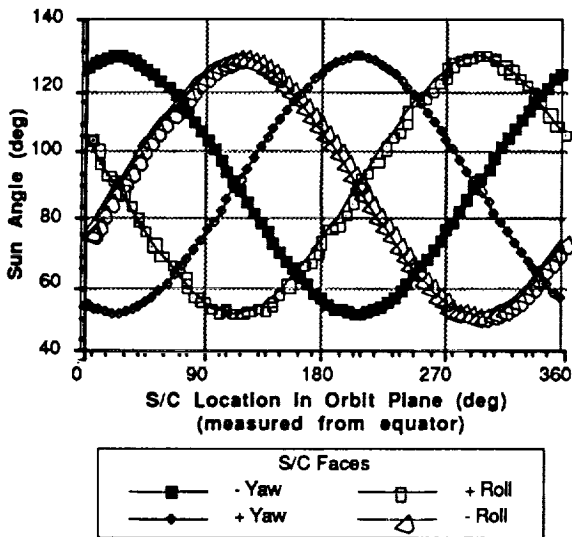


Fig. 5. First day of winter Sun angles on spacecraft faces vs. orbital position (8:30 p.m. ascending node).

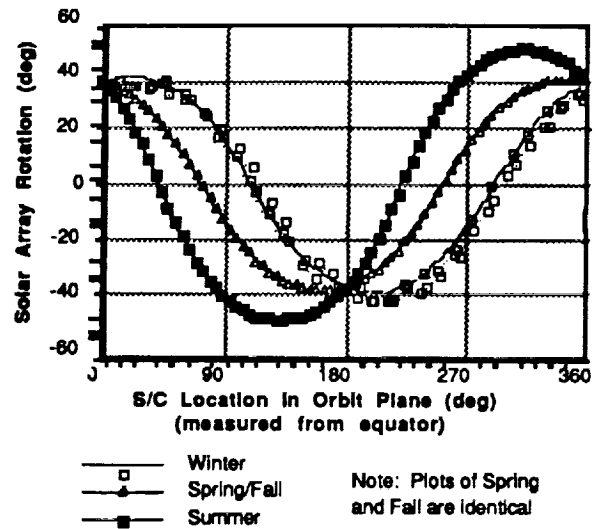


Fig. 7. Solar array rotation angle vs. orbital position and season.

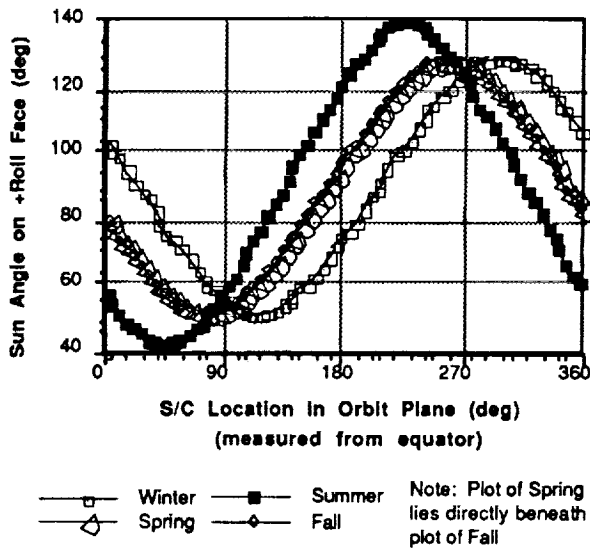


Fig. 6. Sun angle on +roll face vs. orbital position first day of winter (8:30 p.m. ascending node).

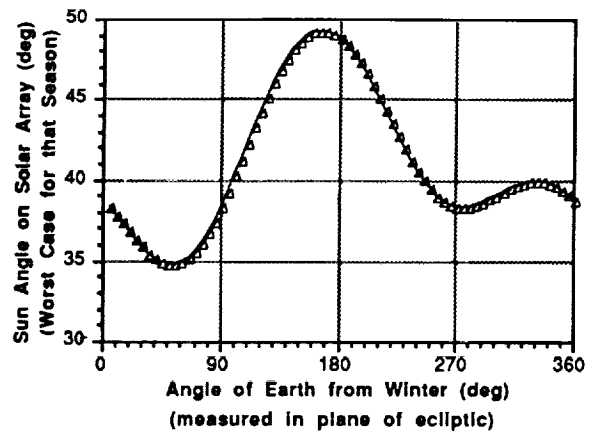


Fig. 8. Worst-case Sun angles vs. time of year.

processing with a Sun sensor or by updated control sequences from the ground.

Eclipse information for the AVHRR mission orbit is required for sizing of the batteries and solar arrays. Eclipse duration for the time of year is shown in Fig. 9.

**EHF Payload Mission**

The analysis of the EHF payload mission does not require the same level of analysis as the AVHRR orbit. The EHF spacecraft is free to rotate about its yaw axis. The satellite is then free

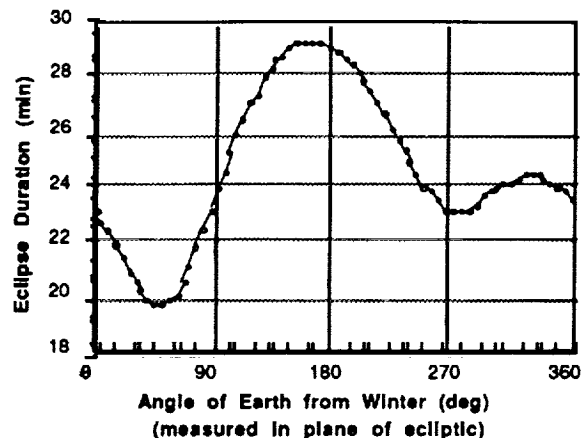


Fig. 9. Eclipse duration vs. time of year.

TABLE 3. Eclipse duration for EHF payload mission.

True Anomaly at Eclipse Entry (deg)	70.587
True Anomaly at Eclipse Exit (deg)	131.715
Eclipse Duration (min)	52.079

to position its solar arrays with zero angle of incidence everywhere in the orbit. The required angle of rotation about the yaw axis, however, has not been examined.

The worst-case eclipse in terms of duration is when the portion of the orbit in eclipse passes directly through the center of the Earth's shadow cylinder. This condition is a function of the longitude of the ascending node. In addition, worst-case eclipse will occur when the portion of the orbit in eclipse is as close to apogee as the geometry will allow. An inclination of 63.43° and an argument of perigee of 270° prevent the apogee from ever entering eclipse. With perigee at the southernmost point in the orbit, the worst-case scenario is created on the first day of winter. The center of the eclipse occurs 113.5° past perigee. Table 3 presents the worst-case eclipse duration.

**ELECTRICAL POWER SUBSYSTEM**

The electrical power subsystem (EPS) consists of solar panels of silicon photovoltaic cells and NiH<sub>2</sub> batteries. Power control electronics will maintain bus voltage at 28 V. The bus will be fully regulated by employing a shunt regulator for periods of solar array operations and will use a boost regulator during periods of battery operations. Table 4 summarizes the power requirements for both the AVHRR and EHF payload missions.

**Solar Array Design**

The MPS bus is designed to have two symmetric solar arrays. The AVHRR and EHF configurations require two solar arrays of two panels each. An additional panel may be added to each side if some future payload requires it; however, only the Taurus SSLV can accommodate the increased volume. Silicon cells were chosen for cost and reliability. The cells selected were the same as those used in INTELSAT VI.

The solar arrays on the EHF payload will be Sun tracking to maintain panel orientation perpendicular to the Sun's rays. This is accomplished through freedom of movement about the longitudinal axis of the arrays and through satellite rotation about the yaw axis. The AVHRR solar panels will, as nearly as possible, be oriented perpendicular to the Sun's rays. The AVHRR operational requirements do not allow for the rotation of the

TABLE 4. System power summaries (normal operations).

Element	AVHRR (W)	EHF (W)
MPS Bus Subtotal	166.4	114.8
Mission Instruments	28.0	115.0
MMS Harness Loss	4.0	4.0
System Reserve	4.0	4.0
Satellite Total	201.8	237.8
With cosine effect	313.9	N/A

TABLE 5. Solar cell characteristics.

Characteristics		K7 Silicon cell	
Power BOL (28°C) (mW)		307.8	
Power EOL (28°C) (mW)		230.8	
BOL			
I <sub>mp</sub> (A)	V <sub>mp</sub> (V)	I <sub>sc</sub> (A)	V <sub>oc</sub> (V)
0.644	0.478	0.6887	0.590
Size (cm)	2.5 × 6.2		
Thickness (cm)	0.02		
Material	Si		
Base Resistivity W-cm/type	10/N/P		
Front junction depth (mm)	0.2		
Back surface field	Yes		
Back surface reflector	Yes		
Contact metallization	TiPdAg		
Front contact width (cm)	0.06		
Anti-reflective coating	TiO <sub>x</sub> Al <sub>2</sub> O <sub>3</sub>		
Cover type	CMX microsheet with anti-reflective coating		
Cover thickness (cm)	0.021		
Cover adhesive	DC 93-500		
Cover front surface	Textured		

TABLE 6. Solar array summary.

	AVHRR	EHF
Number cells series	22	22
Number cells parallel	68	80
Total number cells	1496	1760
Area needed (m <sup>2</sup> )	2.31	2.72
Area available (m <sup>2</sup> )	2.81	2.81

spacecraft about the yaw axis. Therefore, some loss of potential power is introduced from the effect of the angle of incidence, which reaches a maximum of 50°. Using the data from Table 4 and the cell characteristics from Table 5, the actual array panel area was determined and the results summarized in Table 6.

**Battery Design**

The battery for eclipse power is a 12-amp-hr NiH<sub>2</sub> battery manufactured by Eagle Picher. The battery is made in a two-cell common pressure vessel (CPV). Dimensions of each CPV are approximately 8.89 cm (3.5 in) diameter by 15.2 cm (6 in) height. Using a 28-V bus with constant current charge, the number of CPV cells is limited to eight. A NiH<sub>2</sub> battery was chosen because of the high number of charge/discharge cycles the bus may experience. The AVHRR payload, because of its 833 km (450 n.m.) low Earth orbit (LEO), for example, will experience over 15,000 cycles in its three-year design life. The number of charge/discharge cycles the EHF payload will experience may only be 1000. Because the bus was designed to accommodate these and other payloads in various orbits, the battery recharge requirements will vary. For this reason, the recharge circuitry must have the capability to be selectable or be comprised of modular components.

The AVHRR payload configuration draws 100.6 W during eclipse. The recharge rate is determined from the duration of the sunlight period and the amount of power removed. Assuming that 90% of the sunlight period was used to recharge the battery,

the AVHRR charge rate was chosen to be  $C/4$ ; this is only slightly below the maximum recommended charge rate of  $C/3$ , where  $C$  is the battery capacity in amp-hr. This allows for a third of the orbit in eclipse for LEO and a 10% overcharge required for high charge/discharge cycles.

The EHF payload utilizes only 80.7 W during eclipse. Because of the longer sunlight periods and smaller power drawn, the charging rate of this configuration is only  $C/10$ . The battery would be trickle-charged in seasons where the Molniya-type orbit has no eclipse. Table 7 gives the battery summary.

**Radiation Effects**

Radiation effects and shielding requirements were examined for the AVHRR's circular orbit and the EHF's 8-hr Molniya orbit using the JPL Solar Cell Radiation Handbook. The degradation for the AVHRR configuration was based on an annual equivalent of 1 MeV electron fluence assuming solar maximum for the three-year mission. Apogee for the 8-hr Molniya orbit extended into the Van Allen belts, exposing the solar cells to large fluences. Equivalent 1 MeV fluences for 5-min increments of orbital time were calculated for this orbit. Total fluence per orbit, per year, and three-year, lifetime were derived, and the impact on the solar cells calculated. Radiation effects for one year are summarized in Table 8 for both orbits, where  $I_{sc}$  is the short-circuit current, and  $V_{oc}$  is the open-circuit voltage for a solar cell at maximum power ( $P_{max}$ ).

**ATTITUDE CONTROL SUBSYSTEM**

The attitude determination and control subsystem (ADCS) provides precise attitude pointing for the AVHRR or similar payloads in a low 833-km (450 n.m.) circular orbit, and a less accurate determination for the EHF or other communications payload in a Molniya-type orbit. This dual objective is met by using two subsystems for the different requirements, the precision sensor subsystem (PSS) and the basic sensor subsystem (BSS). The PSS and BSS are used for precise positioning, whereas the BSS alone can be used for less stringent requirements. Both subsystems consist of sensors to determine attitude, an onboard processor for control, and an inertial reference system consisting

of an assembly of three orthogonal gyro assemblies (GA). The BSS and PSS share the same components where possible. The attitude control subsystem (ACS) is driven by either the PSS or BSS and consists of three primary reaction wheel assemblies (RWA) with a fourth skewed to provide redundancy, and two magnetic torque rods (MTR) for momentum dumping. Six 0.89-N (0.2 lbf) thrusters can be used for momentum dumping in case of failure of the MTRs or if excessive momentum buildup occurs.

The PSS relies primarily on a celestial sensor assembly (CSA) for attitude determination previously used aboard the DSP Block 5D-3 satellite. The CSA is a strap-down star mapper with a  $10.4^\circ$  field of view. The star sensor measures star transits across a detector and provides an input to the attitude control computer (ACC). The user provides the satellite, approximately once per day, the 80 brightest stars that will be in view of the CSA. The ACC also receives input from the GA and an onboard global positioning system (GPS) receiver. The ACC uses the GPS receiver data and the uplinked catalog to predict star transits that are then compared with actual transits from the CSA to determine attitude error. Gyro drift is then calculated. The inertial attitudes rates from the gyros (corrected for drift in the ACC by the CSA) and the attitudes estimate from the CSA are combined in a Kalman optimal estimation algorithm to provide an attitude determination accuracy of  $0.01^\circ$  as required by the AVHRR payloads. The PSS uses the BSS for backup and initial attitude determination. The GPS receiver provides accurate ephemeris data required by the CSA. Figure 10 shows the PSS block diagram.

The BSS consists of a conical scanning Earth sensor (ES), a digital Sun sensor (DS), the GA, RWAs, ACC, GPS receiver, and MTRs. A scanning ES is required by the wide range of possible altitudes. The ES scans the 14- to 16- $\mu$ m infrared radiance profile of the Earth to determine pitch and roll error, while the DS determines the angle between the pitch axis and the Sun. This information, together with the ephemeris data from the AC and

TABLE 7. Battery summary.

	AVHRR	EHF
Charge required	76.8 W	30.7 W
Charging rate	$C/4$	$C/10$
Charge time	59 min	6.5 hrs
Available sun	64 min	7.1 hrs
Battery capacity	12 A-hr	12 A-hr

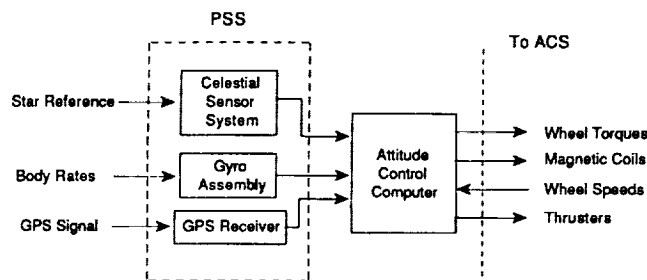


Fig. 10. Functional block diagram of precision sensor subsystem.

TABLE 8. Radiation annual fluence summary (MeV).

	AVHRR		EHF	
	$I_{sc}$	$V_{oc}, P_{max}$	$I_{sc}$	$V_{oc}, P_{max}$
Trapped electrons	$4.59E + 11$	$4.59E + 11$	$3.18E + 13$	$3.18E + 13$
Trapped protons	$8.64E + 12$	$1.47E + 13$	$3.82E + 15$	$1.59E + 15$
Totals	$9.10E + 12$	$1.52E + 13$	$3.85E + 15$	$1.62E + 15$

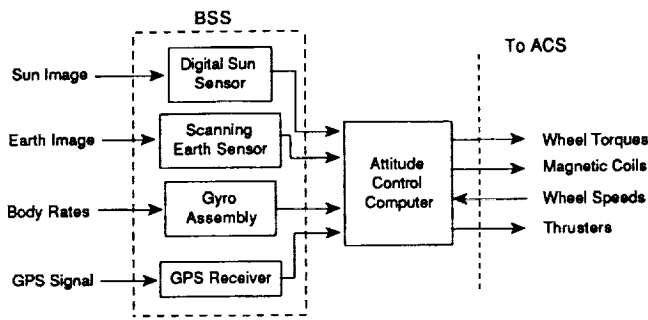


Fig. 11. Functional block diagram of basic sensor subsystem.

GPS receiver, provides yaw error. The BSS can provide better than  $0.5^\circ$  accuracy in each of the three axes. Figure 11 is a functional block diagram of the BSS.

The Attitude Control Subsystem (ACS) is driven by the output of the ACC, which controls the RWAs to correct attitude errors. The RWAs input to the ACC is the load current and wheel speed. The current is used to determine if an overload condition exists, in which case the ACC shuts down the wheel and starts the backup RWA. The wheel speed is used as feedback and to determine if momentum dumping is required. When the momentum reaches the maximum for the wheel, the torque coils are commanded to dump the excess momentum. In case of excessive rate buildup, as determined by differentiators in the circuitry, thrusters are fired to slow the rate to within acceptable limits. The block diagram for the ACS is shown in Fig. 12.

The yaw motion of the satellite in the Molniya-type orbit is modeled as in HILACS<sup>(1)</sup>. This report considers only the attitude control of the meteorological payload. Solar gravity gradient, magnetic, and aerodynamic disturbance torques were modeled in a first-order approximation for the design. The spacecraft was modeled as a rigid body with nonrotating, rigid solar arrays. The equations of motion for a three-axis stabilized

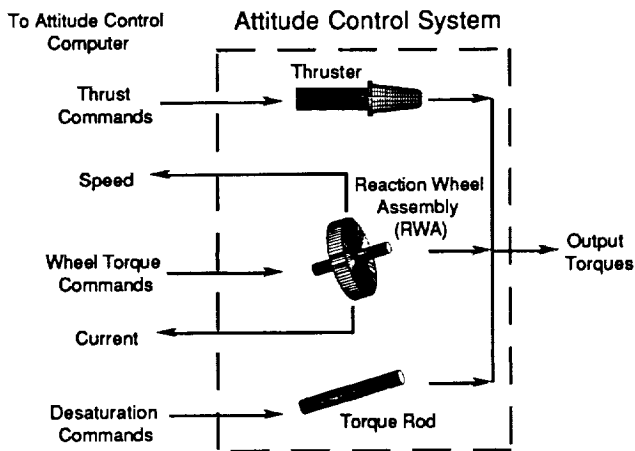


Fig. 12. Functional diagram of attitude control subsystem.

spacecraft were used<sup>(2)</sup> and analysis was done using MATLAB<sup>®</sup> on a PC. Figures 13 through 16 show the resulting error in pitch, roll, and yaw and the pitch wheel speed over one orbit.

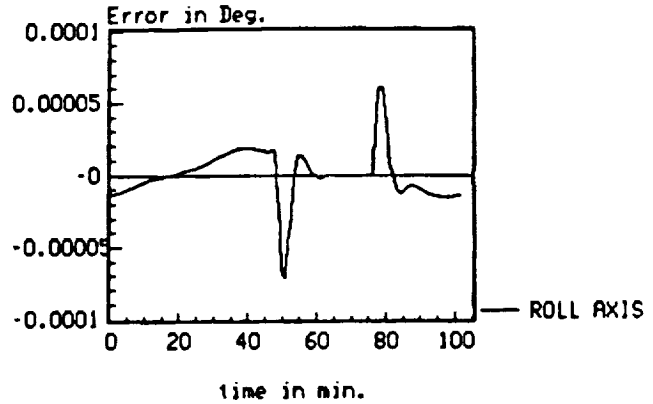


Fig. 13. Roll error for one orbit.

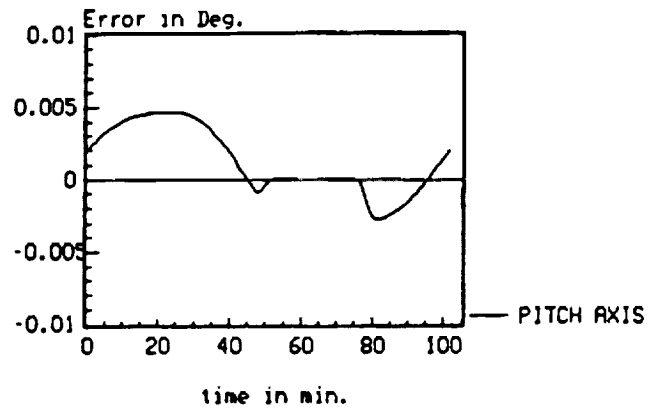


Fig. 14. Pitch error for one orbit.

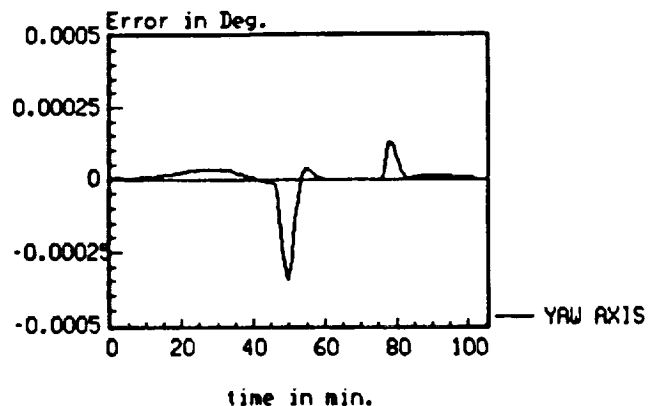


Fig. 15. Yaw error for one orbit.

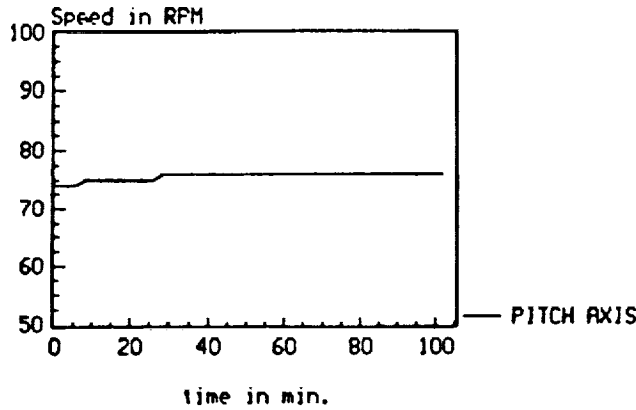


Fig. 16. Pitch wheel speed for one orbit.

The pitch wheel will require periodic desaturation due to the secular torques along the pitch axis (solar and aerodynamic). The pitch MTR will be energized at 250 rpm wheel speed and powered off at 75 rpm. The torque rods will provide a 10-amp-m<sup>2</sup> magnetic dipole that will result in 0.006 N-m of torque over the Earth's geomagnetic poles for the 833 km (450 n.m.) altitude of the circular orbit. The pitch torque rod will be energized within ± 30° of the north and south geomagnetic poles; and the roll-yaw rod (required) powered within ± 30° of the geomagnetic equator. The desaturation scheme for the Molniya-type orbit is dependent upon the longitude of the ascending node. Basically, the roll-yaw rod will be used near the equatorial crossing and the pitch rod near perigee. As can be seen from the plot of the wheel speeds, the pitch wheel gains about 6 rpm for every 5 orbits, resulting in about 17 orbits between MTR cycles. The roll and yaw wheels should not require desaturation due to the cyclic nature of the disturbance torques. The satellite will maintain a 0.01° pointing accuracy during desaturation.

**THERMAL CONTROL SUBSYSTEM**

An initial analysis was conducted to determine the approximate area required to radiate the thermal energy generated based on the power summaries of the spacecraft. The thermal energy dissipated by the EHF payload was estimated to be 148 W and for the AVHRR payload, 115 W. The area required for the EHF payload radiator is 0.48 m<sup>2</sup> (744 in<sup>2</sup>), and 0.37 m<sup>2</sup> (573.5 in<sup>2</sup>) for the AVHRR configuration. It should be noted that the AVHRR assembly has approximately 0.19 m<sup>2</sup> (300 in<sup>2</sup>) in OSR already installed.

Operating temperatures for the solar arrays were calculated for the 2.81 m<sup>2</sup> (30.2 ft<sup>2</sup>) arrays assuming values of 0.8 array absorptance, 0.95 packing efficiency, 0.8 array front emittance, and 0.7 array back emittance. The steady-state operating temperatures for summer solstice and winter solstice are given in Table 9.

Thermal analysis of the spacecraft was done using the PC-ITAS® software package by ANALYTIX Corporation. The model consisted of 145 surfaces for calculating the temperatures at

TABLE 9. Solar array operating temperatures.

T <sub>top</sub>	EHF	HVHRR
Summer Solstice	45.3°C	12°C
Winter Solstice	50.4°C	34.6°C

various points on the spacecraft. The number of nodes was limited to approximately 165 by the amount of memory on the computer. This was deemed sufficient for this preliminary design. The analysis considered only steady-state temperatures for the two different orbits.

This preliminary analysis indicates that, with proper selection of coatings and materials, the temperatures of the various equipment can be maintained within operating ranges. There are specific nodes that are too cold or too hot, but, since these are identified, corrective action can be implemented. Corrective action in these cases would be to insulate or link by conduction the equipment to the radiator.

**PROPULSION SUBSYSTEM**

The propulsion subsystem consists of six 0.89-N (0.2 lbf) thrusters made by Rocket Research Corporation (model number MR103C), a 0.41-m (16 in) diameter tank made of titanium alloy manufactured by TRW Pressure Systems, Inc., one pressure transducer, and one pressure regulator to monitor the pressure throughout the system. The MR103C minimizes space required for mounting. The MR103C is also the lightest of the 0.89-N thrusters considered. An 8-μm filter is incorporated to screen the impurities remaining in the fuel.

The system is installed primarily as a backup system for reaction wheel desaturation, orbit maintenance, and orbit stationkeeping, and has no redundancy. The propulsion system will be used to correct minor errors in the orbit after separation. On orbit, the system will provide ΔV for stationkeeping. Figure 17 shows a schematic of the propulsion subsystem. Figure 18 shows the placement of thrusters on the MPS bus.

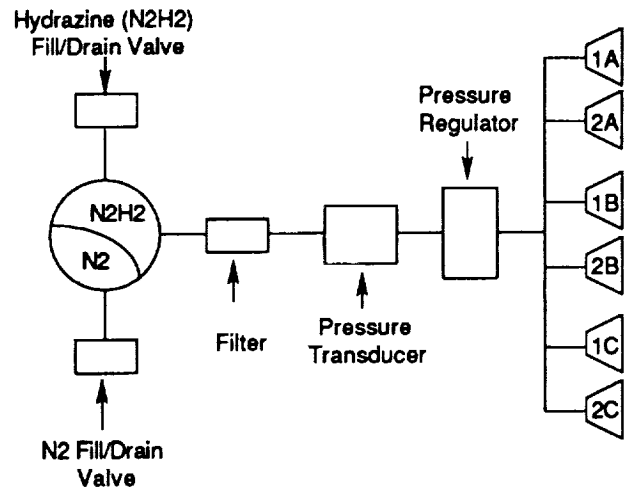


Fig. 17. Propulsion subsystem schematic.

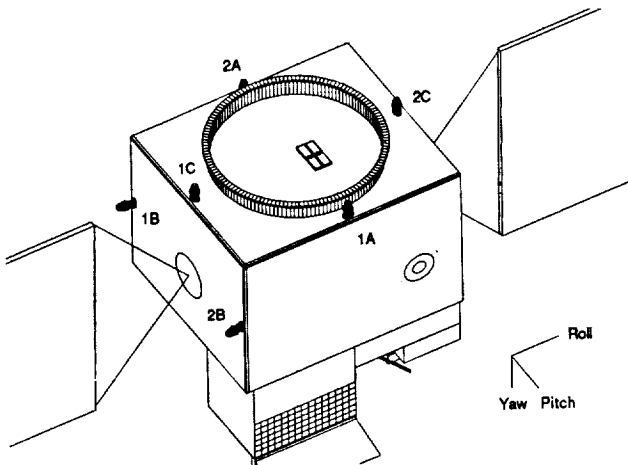


Fig. 18. Location of thrusters.

Thruster operations can be performed with or without the solar arrays deployed to desaturate the reaction wheels along any axis.  $\Delta V$  maneuvers can only be provided in the +yaw or the +roll directions. The positive roll thrusters are placed to provide  $\Delta V$  for orbit maintenance without the need for reorientation of the spacecraft. Major orbit changes will require reorientation of the spacecraft to align the flight path of the spacecraft along the +z axis. Deactivation of some equipment may be required for major orbit corrections. The two thrusters along the east face could possibly impinge on the solar panels, depending on the angular position of the arrays. An electronic cutout cam would have to be installed to prevent accidental firing and subsequent damage to the arrays. It is unlikely that this would affect AVHRR operations as the arrays operate  $\pm 50^\circ$  of the roll/yaw plane. The EHF payload may require the arrays to rotate  $\pm 90^\circ$  roll/yaw plane necessitating close management of solar array and thruster operations. The thrusters along the positive roll axis are canted out at an angle of  $8^\circ$  as an additional precaution.

**TELEMETRY, TRACKING, AND COMMAND**

The telemetry, tracking, and command (TT&C) package for the MPS bus is designed to be compatible with the Air Force Space-Ground Link Subsystem (SGLS) for satellite control. TT&C is designed in the bus to operate at super-high frequencies (SHF) that correspond to channel 1 of the SGLS ground terminal as given in Table 10.

The TT&C package sends and receives data from the payload and/or the anti-Earth-face antenna through command-controlled switches that allow the ground terminal to shift between payload

TABLE 10. TT&C operating frequencies.

Command Uplink:	1.763721 GHz
Telemetry Downlink:	2.2 GHz
Carrier 1:	2.2025 GHz
Carrier 2:	2.1975 GHz

antennas and the anti-Earth-face antenna. The anti-Earth-face antenna is a four-element microstrip antenna that uses the same elements as the AVHRR antenna and has a gain of 2.5 dB. The switches may be aligned such that during launch and activation, TT&C will be accomplished with the SGLS system channel 1 to the anti-Earth-face antenna. The payload TT&C is activated and the anti-Earth-face telemetry downlink is put on standby once the satellite is on station. The anti-Earth-face command receiver will remain active in case the satellite attitude control system fails.

The remote tracking unit (RTU) takes commands from the antennas and payloads in the SGLS format and demodulates and decodes them for the remote command unit (RCU) on up-link. The RTU also modulates and encodes telemetry signals from the RCU for down-link. The RTU block diagram is shown in Fig. 19.

The RCU receives a command from the RTU and passes it to the microprocessor for command recognition and execution. Data is gathered from all sensors and the payload and compiled into a telemetry down-link signal for the RTU. The signal uses frequency-shift-key (FSK) modulation to avoid phase ambiguities, and will be encoded to provide some error correction. Figure 20 shows the block diagram of the RCU.

A global positioning system (GPS) receiver is used for tracking below 20,000 km altitude. The satellite will most likely be receiving lower-powered side-lobes requiring significant antenna gain in order to achieve the 34 dB C/N ratio needed to receive analog data. A tracking beacon in the RCU can be turned on

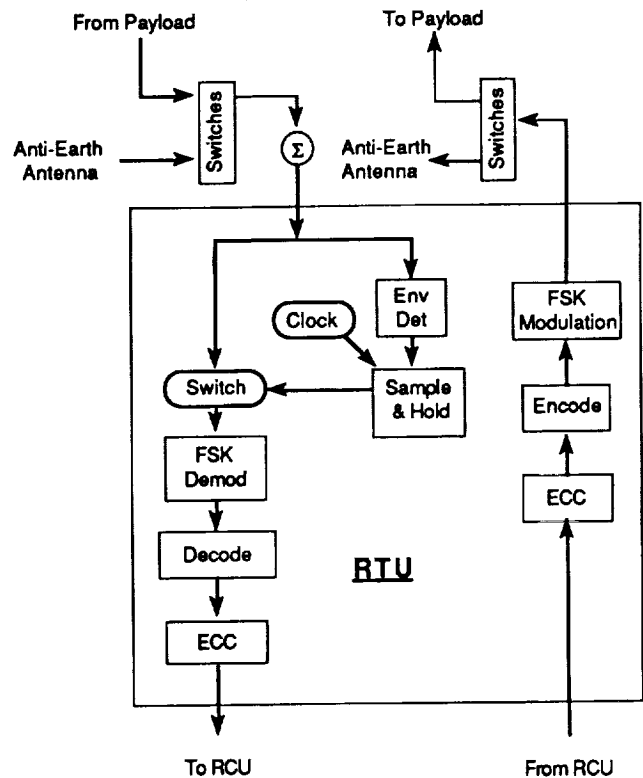


Fig. 19. Remote tracking unit.

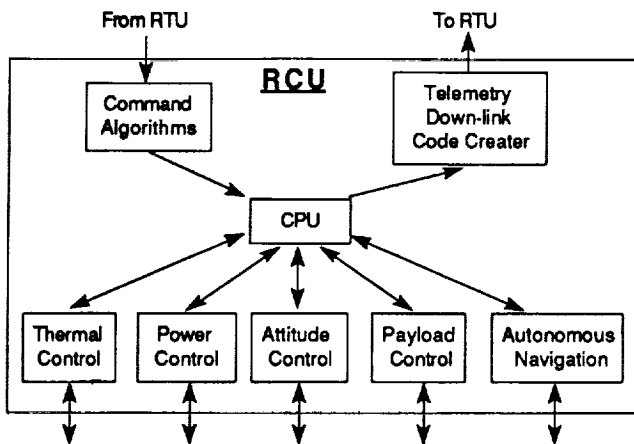


Fig. 20. Remote command unit.

with a command signal, and manual range and range rate tracking can be accomplished in the event the GS receiver is not accurately predicting the position of the satellite. The tracking beacon is intended for standby use allowing 15.2 m (50 ft) and 0.037 m/s (0.120 ft/s) resolution.

**STRUCTURE DESIGN**

The spacecraft bus structure is designed to fit within the 1.17-m (46 in) diameter Pegasus shroud with two folding solar panels and within the Taurus shroud with three, if required. A rectangular design was chosen for simplicity and ease of assembly. The bus is built on a rectangular frame that is composed of hollow rectangular cross-section tubing made from 6061-T6 aluminum. Five load-supporting honeycomb panels with aluminum faceskins are attached to the frame, one being the anti-Earth face. The sixth side of the spacecraft bus is the Earth/payload face. The entire spacecraft is mounted to Pegasus with a standard Marmon clamp assembly. Total weight of the dry standard bus structure is 20.4 kg (45 lb) for the AVHRR configuration and 26.8 kg (59 lb) for the EHF configuration. Launch design accelerations are given in Table 11. The structure margins of safety for the various components are given in Table 12.

TABLE 11. Accelerations at payload interface [m/s<sup>2</sup>].

Flight Mode	X (Roll)	Y (Pitch)	Z (Yaw)
Captive Carry	+8.82	+8.06	+34.3
	-6.66	-9.04	-13.7
Powered Flight	+0	+4.9	+27.4
	-83.3	-4.9	-9.8

TABLE 12. Margins of safety.

Component Mix Load	Expected	Yield Load of Safety	Margin
Aluminum Frame	6.2E06 Pa [900 psi] (compression)	255.1E06 Pa [37,000 psi]	32
Aluminum Frame	86.9E06 Pa [12,600 psi] (bending)	255.1E06 Pa [37,000 psi]	1.9
Aluminum Frame	6.89E06 Pa [1,000 psi] (shear)	206.8 Pa [30,000 psi]	29
Honeycomb Panel	196 m/s <sup>2</sup> [20 g]	255.1E06 Pa [37,000 psi]	1.1
Honeycomb Panel	78.6E06 Pa [11,406 psi] (facing stress)	165.5E06 Pa [24,000 psi]	1.1

**ACKNOWLEDGMENTS**

The 1990 design project team would like to thank B. Agrawal for his guidance and assistance throughout the 11-week quarter. His continuous support was sincerely appreciated and ensured the success of the project. We are also indebted to G. Myers, T. Ha, D. Wadsworth, and R. Adler of the Naval Postgraduate School, who consistently made themselves available to answer our questions. M. Brown, C. Merk, S. Coffey, M. Zedd, R. Morris, P. Carey, and N. Davinic of the Naval Research Laboratory also contributed to the success of the project. W. Cummings of MIT Lincoln Laboratory and L. Flinn, R. Sudol, and P.-A. Stiffler of Space Applications also made significant contributions. Finally we appreciate the continued interest of J. Burke, our NASA representative from the Jet Propulsion Laboratory.

**REFERENCES**

1. National Oceanic and Atmospheric Administration Technical Report NESDIS, *Final Report on the Modulation and EMC Considerations for the HPRP Transmission System in the Post NOAA-M Polar Orbiting Satellite Era*, U. S. Dept. of Commerce, Washington D. C., June 1989.
2. Agrawal B. M., *Design of Geosynchronous Spacecraft*, Prentice-Hall, 1986.
3. Lindberg R. E., "Brief to the Space Test Program Tri-Service Experiment Review," 9 May 1989.